OPTIMUM - OPTIMORUM INTEGRATED WING-FUSELAGE CONFIGURATION FOR SUPERSONIC TRANSPORT AIRCRAFT OF SECOND GENERATION

ICAS-86-1.3.6

Adriana Nastase
Lehrgebiet Aerodynamik des Fluges
Rheinisch-Westfälische Technische Hochschule Aachen, Germany

Abstract

The author presents an original, hybrid, analytical-numerical method for the design of the optimum-optimorum shape of the integrated wing fuselage configuration, for which all its geometrical characteristics (i.e. cambers, twists, thicknesses and also the planprojections of the wing and of the fuselage) are simultaneously determined in order to obtain a minimum drag, at cruising Mach number M_∞. The design of the optimum-optimorum shape of the integrated wing-fuselage configuration needs 5 seconds computer time, on Cyber 175.

I. Introduction

Previous theoretical considerations of the author [(1)-(10)], lead to the conclusion that the drag of supersonic aircraft can be greatly reduced if the conventional wings are replaced with fully-optimized delta wings (called by the author optimum-optimorum delta wings).

The next step of the drag reduction of the entire aircraft is to design optimum-optimorum shapes of integrated wing-fuselage configurations.

A wing-fuselage configuration is here considered as a wing alone, which surface is discontinuous along the junction lines between the wing and the fuselage. If, additionally, the wing and the fuselage have the same tangent surfaces in each point of their junction lines, the equivalent wing of the wing-fuselage configuration is here called integrated wing.

The design of optimum-optimorum integrated wing leads to the solving of two mathematical problems.

- The first problem consists in the determination of the solution of a three-dimensional boundary value problem for the dimensionless axial disturbance velocity u on the wing-fuselage configuration.

The downwash w is supposed to be piecewise approximated in form of superposition of homogeneous polynoms in two variables.

The solution given here by the author for u in integrated form fulfils a three-dimensional hyperbolic partial differential equation and the boundary conditions on the wing and fuselage, at the infinity (forward) and also on the characteristic Mach cone of the apex of the wing-fuselage configuration. Additionally, this solution for u is matched with a boundary layer solution. This solution for u is obtained by using the results of high conical flow theory of Germain [(11)], the hydrodynamic analogy of Carafoli [(12),(13)] and the principle of minimum singularities [(14),(15)].

- The second mathematical problem consists in the determination of the optimum-optimorum shape of the integrated wing.

The determination of this shape leads to the solving of an extended variational problem for the drag functional $C_d^{(t)}$, which consists in the simultaneous determination of the equations $Z^{(t)}(x_1,x_2)$ and $Z'^{(t)}(x_1,x_2)$ of the shapes of wing and fuselage surfaces (which enter as unknown functions in the drag functional $C_d^{(t)}$) and of the similarity parameters ν and $\bar{\nu}$ of the planprojections of wing and fuselage (which enter in the boundary of the drag functional $C_d^{(t)}$) in such a manner that the drag attains its minimum, for a given cruising Mach number M_∞.

An original hybrid, numerical-analytical method (called also graphic-analytical method), is here presented in order to approach the solution. The graphic-analytical method is a further application of the optimum-optimorum theory of the author [(6)], which will be presented below.

II. The Optimum - Optimorum Theory for Integrated Wings

The optimum-optimorum theory was introduced by the author [(2),(3),(4),(5),(6)] for the wing alone. It allows also the determination of the here called optimum-optimorum integrated wing among a given class of integrated wings. The integrated wings belonging to a class are defined by means of their geometrical and aerodynamical properties.

Two integrated wings belong to the same class if:
- their planforms can be related through affine transformations. Both planforms are defined by the same number of free similarity parameters ($\nu_1,\nu_2,..\nu_n$) with the same significance;
- their surfaces are piecewise generated (or approximated) in the form of superpositions of homogeneous polynoms of the same degrees. The coefficients of these polynoms are free parameters;
- the integrated wings satisfy the same auxiliary conditions.

In order to solve this enlarged variational problem for the drag-functional $C_d^{(t)}$ (of the optimum-optimorum integrated wing) with free boundary the author uses its hybrid, graphic-analytical method [(2),(3),(4),(5),(6)], which reduces the computer time necessary for the determination of the fully-optimized shape of the integrated wing. This method starts for the remark that the dependance of the drag functional $C_d^{(t)}$ versus the coefficients of the polynoms (which approximate the surfaces of the integrated wing) is of quadratic form, while the dependance versus the similarity parameters of the planform are nonlinear and very complicated.

The method presents two steps.
- In the first step the set of similarity parameters of the planform ($\nu_1,\nu_2,..,\nu_n$) are considered as given. The boundary of the drag functional $C_d^{(t)}$ is now a priori known. The optimal values of the coefficients of polynomial expansions of the surface of the integrated wing are obtained by solving a linear, algebraic system. These optimal coefficients determine uniquely the value of the drag functional $C_d^{(t)}$, for the prescribed set of similarity parameters of the planform.
- In the second step, through systematical variation of the set of similarity parameters, each point of what is termed here lower-limit hypersurface of the drag functional $C_d^{(t)}$ i.e.

$$(C_d^{(t)})opt = f(\nu_1, \nu_2,..,\nu_n), \qquad (1)$$

can be analytically determined. The "position" of the minimum of the hypersurface is determined numerically (or graphically) and gives the best set of similarity parameters $(\nu_1,\nu_2,..,\nu_n)$ of the planform, as presented in Fig.1, for two similarity parameters.

The optimal set of similarity parameters together with a chosen area S_0 of the planprojection determine the shape of the planform of the optimum-optimorum integrated wing of the class. The optimum-optimorum integrated wing is exactly this optimal integrated wing (corresponding to this optimal set of similarity parameters). The minimum value of the "ordinate" of the hypersurface represents the drag coefficient of the optimum-optimorum integrated wing of the class.

The above theory was previously used by the author (3)-(10) and (18) for the effective design of the shape of optimum-optimorum delta wing Adela, presented in Fig.2. This wing has a minimum drag at cruising Mach number $M_\infty = 2$ and presents a low drag and a high lift for a great range of Mach numbers and angles of attack.

For the effective design of the optimum-optimorum shape of the integrated delta wing it is firstly necessary to solve the boundary value problem for the axial disturbance velocity u of the wing-fuselage configuration.

III. Determination of the Solution of the Three - Dimensional Boundary Value Problem of the Axial Disturbance Velocity u of the Integrated Delta Wing

Let us refer the integrated thick, lifting delta wing to a three-orthogonal system of axes $Ox_1x_2x_3$ having the apex O of the wing as origin. The plane Ox_1x_3 is the plane of symmetry of the integrated wing and the axis Ox_1 is the bisectrix of the angle of the integrated wing, in the plane Ox_1x_3, at its apex (the shockfree entry direction).

The integrated thick, lifting delta wing surface is supposed to be flattened in the plane Ox_1x_2 presented in Fig.3a.

The integrated thick, lifting delta wing is considered in a parallel stream with the undisturbed velocity $\vec{v}_\infty$, at moderate angle of attack α (measured between the Ox_1- axis and $\vec{v}_\infty$).

In the framework of linearised theory for flattened integrated thick, lifting delta wings at moderate angle of attack α, in the boundary value problem concerning the determination of the axial disturbance velocity u the effect of lift can be separated from the effect of thickness.

Further the following two delta wing components will be separately considered:

- the thin integrated delta wing which is the skeleton surface of the thick, lifting integrated delta wing and is considered at the same angle of attack α and,
- the thick-symmetrical integrated delta wing which has the same thickness distribution as the thick, lifting integrated delta wing, but its skeleton surface is plane. This component is considered at zero angle of attack.

The skeleton surface $Z(x_1,x_2)$ of the integrated delta wing is supposed to be continuous, but, for the sake of generality, the thickness distributions $Z^*(x_1,x_2)$ on the lateral sides OA_1C_1 and OA_2C_2 (corresponding to the wing) and $Z'^*(x_1,x_2)$ on the central part OC_1C_2 (corresponding to the fuselage) are supposed to be different. Further this wing will be called initial integrated delta wing.

The author introduced, (2),(3),(4),(5) a well-suited affine transformation in order to obtain dimensionless coordinates

$$\tilde{x}_1 = \frac{x_1}{h_1}\ , \quad \tilde{x}_2 = \frac{x_2}{\ell_1}\ , \quad \tilde{x}_3 = \frac{x_3}{h_1} \tag{2}$$

$$\left(\tilde{y} = \frac{y}{\ell}\ ,\ \ell = \frac{\ell_1}{h_1}\ ,\ \nu = B\,\ell\ ,\ \bar{\nu} = B\,c'\ ,\ B = \sqrt{|M_\infty^2 - 1|}\right)$$

A transformed integrated delta wing is obtained, which has the maximal depth $\tilde{1}$ and the half-span 1 (Fig.3b). The traces $\tilde{C}_1$ and $\tilde{C}_2$ of the junction lines $\tilde{O}\tilde{C}_1$ and $\tilde{O}\tilde{C}_2$ (between the wing and the fuselage) have the following positions on the axis $\tilde{C}\tilde{y}$ (parallel to axis $\tilde{O}\tilde{x}_2$) $\tilde{y}_c = \pm\,\bar{\nu}/\nu$.

The transformed integrated delta wing is placed in a supersonic flow with the cruising Mach number $\tilde{M} = \sqrt{1 + \nu^2}$.

The skeleton surface $\tilde{Z}(\tilde{x}_1,\tilde{x}_2)$ of the transformed

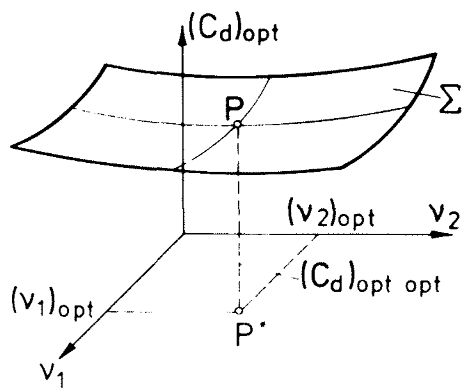

Fig.1 The Lower-Limit Hypersurface (Σ)

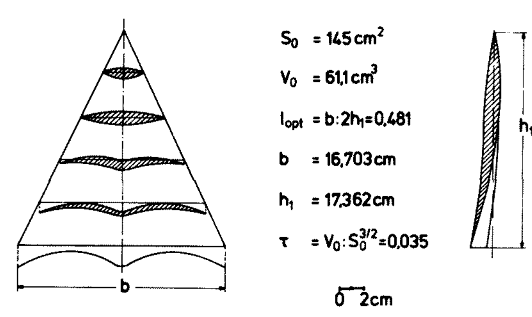

Fig.2 The Optimum-Optimorum Delta Wing Adela

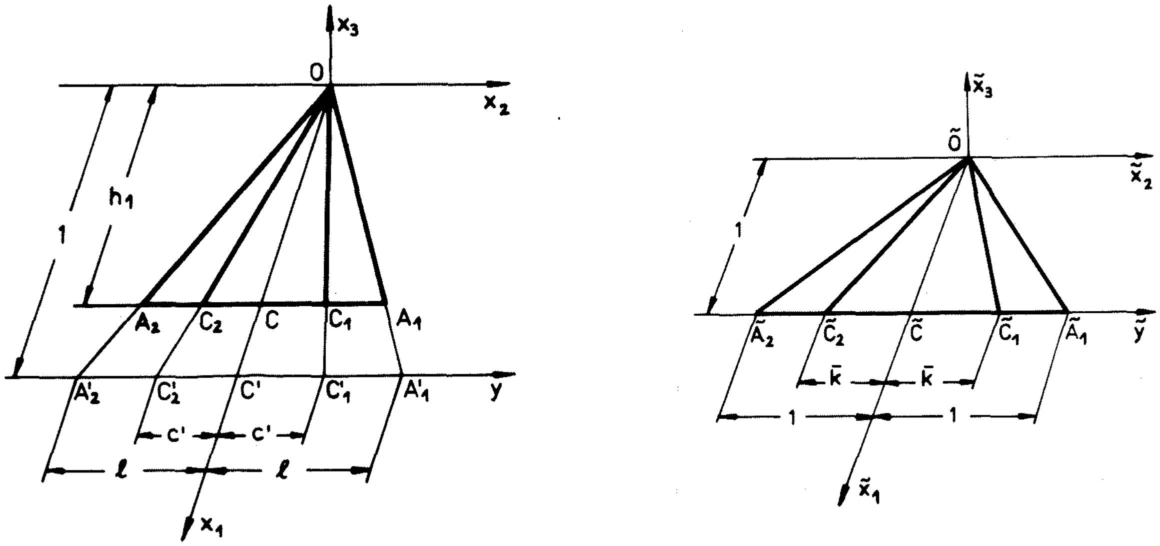

Fig.3a,b Initial and Transformed Integrated Wings

integrated delta wing is also continuous but the thickness distributions $\tilde{Z}^*(\tilde{x}_1,\tilde{x}_2)$ and $\bar{Z}^*(\tilde{x}_1,\tilde{x}_2)$ on the lateral sides $\tilde{O}\tilde{A}_1\tilde{C}_1$ and $\tilde{O}\tilde{A}_2\tilde{C}_2$ (corresponding to the wing) and $\tilde{O}\tilde{C}_1\tilde{C}_2$ (corresponding to the fuselage) are different.

Between the equations of the skeletons $Z(x_1,x_2)$ and $\tilde{Z}(\tilde{x}_1,\tilde{x}_2)$ and the thickness distributions $Z^*(x_1,x_2)$, $Z'^*(x_1,x_2)$ and $\tilde{Z}^*(\tilde{x}_1,\tilde{x}_2)$, $\bar{Z}^*(\tilde{x}_1,\tilde{x}_2)$ (in corresponding points through the transformation (2)) of the initial and transformed integrated delta wing components there are the following relations

$$Z = h_1\,\tilde{Z}\quad,\quad Z^* = h_1\,\tilde{Z}^*\quad,\quad Z'^* = h_1\,\bar{Z}^* \tag{3}$$

Between the dimensionless axial disturbance velocities u, u^* and $\tilde{u}$, $\tilde{u}^*$ and the dimensionless downwashes w, w^*, w'^* and $\tilde{w}$, $\tilde{w}^*$, $\bar{w}^*$ of the initial and transformed integrated delta wing components there are the following relations:

$$u = \ell\,\tilde{u}\quad,\quad w = \tilde{w}\quad, \tag{4a}$$

$$u^* = \ell\,\tilde{u}^*\quad,\quad w^* = \tilde{w}^*\quad,\quad w'^* = \bar{w}^* \tag{4b}$$

Further the assumption is made that the downwashes $\tilde{w}$, $\tilde{w}^*$ and $\bar{w}^*$ are expressed in form of superpositions of homogeneous polynomes in $\tilde{x}_1$ and $\tilde{x}_2$ i.e.
- for the thin component of the transformed integrated wing

$$\tilde{w} = \sum_{m=1}^{N} \tilde{x}_1^{m-1} \sum_{k=0}^{m-1} \tilde{w}_{m-k-1,k}\,|\tilde{y}|^k \tag{5}$$

- for the thick-symmetrical component of the transformed integrated wing, if $\bar{k} < |\tilde{y}| < 1$

$$\tilde{w}^* = \sum_{m=1}^{N} \tilde{x}_1^{m-1} \sum_{k=0}^{m-1} \tilde{w}^*_{m-k-1,k}\,|\tilde{y}|^k \tag{6}$$

and

$$\bar{w}^* = \sum_{m=1}^{N} \tilde{x}_1^{m-1} \sum_{k=0}^{m-1} \bar{w}^*_{m-k-1,k}\,|\tilde{y}|^k, \tag{7}$$

if $|\tilde{y}| < \bar{k}$. Here $\bar{k} = \bar{\nu}/\nu$ is supposed to be constant.

The coefficients $\tilde{w}_{ij}$, $\tilde{w}^*_{ij}$ and $\bar{w}^*_{ij}$ and the similarity parameter ν are unknown and will be determined through the fully-optimization process.

The axial disturbance velocity $\tilde{u}$ on the thin component of the transformed integrated thick, lifting delta wing, which has eventually also a central ridge, according to (2),(3),(4),(16), is of the form

$$\tilde{u} = \sum_{n=1}^{N} \tilde{x}_1^{n-1} \left\{ \sum_{q=0}^{E(\frac{n}{2})} \frac{\tilde{A}_{n,2q}\,\tilde{y}^{2q}}{\sqrt{1-\tilde{y}^2}} + \sum_{q=1}^{E(\frac{n-1}{2})} \tilde{C}_{n,2q}\,\tilde{y}^{2q}\cosh^{-1}\sqrt{\frac{1}{\tilde{y}^2}} \right\}. \tag{8}$$

and the axial disturbance velocity $\tilde{u}^*$ of the thick-symmetrical component of the transformed integrated thick, lifting delta wing is, as in (2),(3),(5),(17),

$$\begin{aligned}\tilde{u}^* = \sum_{n=1}^{N} \tilde{x}_1^{n-1} \Bigg\{ & \sum_{q=0}^{E(\frac{n}{2})} \frac{\tilde{P}^*_{n,2q}\,\tilde{y}^{2q}}{\sqrt{1-\nu^2\tilde{y}^2}} + \sum^{n-1} \tilde{G}^*_{nq}\,\tilde{y}^q \left[\cosh^{-1}R_1 + (-1)^q\cosh^{-1}R_2\right] + \\ & + \sum_{q=0}^{n-1} \tilde{H}^*_{nq}\,\tilde{y}^q \left[\cosh^{-1}M_1 + (-1)^q\cosh^{-1}M_2\right] + \\ & + \sum_{q=1}^{E(\frac{n-1}{2})} \tilde{C}^*_{n,2q}\,\tilde{y}^{2q}\cosh^{-1}\sqrt{\frac{1}{\nu^2\tilde{y}^2}} \Bigg\}.\end{aligned} \tag{9}$$

Here the following notations will be made

$$R_1 = \sqrt{\frac{(1+\bar{\nu})(1-\nu\tilde{y})}{2(\bar{\nu}-\nu\tilde{y})}}\qquad R_2 = \sqrt{\frac{(1+\bar{\nu})(1+\nu\tilde{y})}{2(\bar{\nu}+\nu\tilde{y})}} \tag{10a}$$

and

$$M_1 = \sqrt{\frac{(1+\nu)(1-\nu\tilde{y})}{2\nu(1-\tilde{y})}} \quad M_2 = \sqrt{\frac{(1+\nu)(1+\nu\tilde{y})}{2\nu(1+\tilde{y})}} \tag{10b}$$

The coefficients of $\tilde{u}$ for the thin transformed integrated delta wing are related to the coefficients of the downwashes $\tilde{w}$ and the coefficients of $\tilde{u}^*$ for the thick-symmetrical transformed integrated delta wing are related to the coefficients of the downwashes $\tilde{w}^*$ and $\bar{w}^*$ through the following linear and homogeneous relations

$$\tilde{A}_{n,2q} = \sum_{j=0}^{n-1} \tilde{a}^{(n)}_{2q,j}\, \tilde{w}_{n-j-1,j} \tag{11}$$

$$\tilde{P}^*_{n,2q} = \sum_{j=0}^{n-1} (\tilde{p}^{*(n)}_{2q,j}\, \tilde{w}^*_{n-j-1,j} + \bar{p}^{*(n)}_{2q,j}\, \bar{w}^*_{n-j-1,j}) \tag{12}$$

The constants $\tilde{a}^{(n)}_{2q,j}$, $\tilde{p}^{*(n)}_{2q,j}$, $\bar{p}^{*(n)}_{2q,j}$ etc. are functions only of the similarity parameter ν.

IV. The Variational Problem of the Optimum-Optimorum Thick, Lifting Integrated Delta Wing

The variational problem concerning the determination of the optimum-optimorum shape of the thick, lifting integrated delta wing leads to the determination of the coefficients $\tilde{w}_{ij}$ and $\tilde{w}^*_{ij}$, $\bar{w}^*_{ij}$ of the downwashes $\tilde{w}$ and $\tilde{w}^*$, $\bar{w}^*$ (of the thin and, respectively, thick-symmetrical delta wing component) and of the similarity parameter ν of the planprojection in such a manner that the drag functional $C_d^{(t)}$ of the thick, lifting integrated delta wing presents a minimum (at cruising Mach number M_∞). The integrated delta wing must additionally satisfy the following auxiliary conditions:
- the lift and pitching moment coefficients C_ℓ, C_m are given and the axial disturbance velocity u (of the thin wing component) must cancel along the leading edges of the wing in order to avoid the birth of leading edge vortices and to cancel the induced drag (at cruising Mach number). It results:

$$C_\ell = C_{\ell_0} \quad , \quad C_m = C_{m_0} \quad , \quad u_{y \to \ell} = 0 \tag{13a,b,c}$$

- the relative volumes τ and τ' of the wing and fuselage are given:

$$\tau = \tau_0 \quad , \quad \tau' = \tau'_0 \tag{14a,b}$$

- the surface of the integrated wing has zero-thickness along the leading edges

$$Z^*(x_1 , y = \ell) = 0; \tag{15}$$

- the surface of the integrated wing must be continuous of class C_1 along the junction line between the wing and fuselage

$$Z^*(x_1 , y = c') = Z'^*(x_1 , y = c'), \tag{16a}$$

$$Z^*_{x_1}(x_1 , y = c') = Z'^*_{x_1}(x_1 , y = c'), \tag{16b}$$

$$Z^*_{x_2}(x_1 , y = c') = Z'^*_{x_2}(x_1 , y = c'), \tag{16c}$$

- the surface of the integrated wing is of zero-thickness along the trailing edge

$$Z^*(x_1 = h_1 , x_2) = 0 \quad , \quad Z'^*(x_1 = h_1 , x_2) = 0 \tag{17a,b}$$

The auxiliary conditions (13a,b,c) concern only the thin integrated wing component and the auxiliary conditions (14a,b)-(17a,b) affect only the thick-symmetrical integrated wing component.

Taking also into account that, in the frame of linearised theory, the interference drag between the wing components vanishes, the drag $C_d^{(t)}$ of the thick, lifting integrated wing is to be obtained through the addition of the drag C_d and C_d^* of the thin and thick-symmetrical integrated wing components i.e.

$$C_d^{(t)} = C_d + C_d^* . \tag{18}$$

If the classical variational problem concerning the optimization of the shape of the surface of the integrated thick, lifting wing with given planprojection (and therefore with given similarity parameter ν) is firstly considered, it is possible to split it into two independent variational problems concerning the wing components, i.e.
- the variational problem concerning the determination of the shape of the surface of the thin integrated delta wing component in order to obtain

$$C_d = \min. \tag{19}$$

with the auxiliary conditions (13a,b,c);
- the variational problem related with the determination of the shape of the surface of the thick-symmetrical integrated wing component in such a manner that

$$C_d^* = \min. \tag{20}$$

with the auxiliary conditions (14a,b),(15),(16a,b,c) and (17a,b).

The classical variational problem concerning the optimization of the wing components, for a given value of the similarity parameter ν, shall be firstly treated. After that, the graphic-analytical method for the performing of the fully-optimization of the thick, lifting integrated delta wing will be presented.

V. Determination of the Optimum Shape of the Thin Integrated Delta Wing

The determination of the optimum shape of the thin integrated delta wing components leads to the determination of the values of coefficients $\tilde{w}_{ij}$ in such a manner that the drag coefficient C_d reaches its minimum and the auxiliary conditions (13a,b,c) are satisfied.

According to the formulas (2)-(9), between the aerodynamic characteristics of the initial and the transformed thin integrated wings there exists the following relations

$$C_\ell = \ell\, \tilde{C}_\ell \quad , \quad C_m = \ell\, \tilde{C}_m \quad , \quad C_d = \ell\, \tilde{C}_d . \tag{21}$$

The auxiliary conditions (13a,b,c) can be written in the following form for the transformed integrated thin wing:
- the given coefficient C_ℓ

$$\tilde{C}_\ell \equiv \sum_{n=1}^{N} \sum_{j=0}^{n-1} \tilde{\Lambda}_{nj}\, \tilde{w}_{n-j-1,j} = \frac{C_{\ell_0}}{\ell} \tag{22}$$

- the given pitching moment C_m

$$\tilde{C}_m \equiv \sum_{n=1}^{N} \sum_{j=0}^{n-1} \tilde{\Gamma}_{nj}\, \tilde{w}_{n-j-1,j} = \frac{C_{m_0}}{\ell} \tag{23}$$

- the cancellation of the axial disturbance velocity u along the leading edges

$$\tilde{F}_t \equiv \sum_{j=0}^{E(\frac{t}{2})} \tilde{\psi}_{tj}\ \tilde{w}_{t-j-1,j} = 0 \tag{24}$$

$(t = 0,1,\ldots, (N-1)\ )$.

The drag coefficient C_d of the thin integrated delta wing takes the following form

$$C_d = \ell \sum_{n=1}^{N}\sum_{m=1}^{N}\sum_{k=0}^{m-1}\sum_{j=0}^{n-1} \tilde{\Omega}_{nmkj}\ \tilde{w}_{m-k-1,k}\ \tilde{w}_{n-j-1,j} \tag{25}$$

The expressions $\tilde{\Lambda}_{nj}$, $\tilde{\Gamma}_{nj}$, $\tilde{\psi}_{tj}$ and $\tilde{\Omega}_{nmkj}$ depend only on the similarity parameter ν.

The variational problem concerning the determination of the minimum of the drag functional C_d with the auxiliary conditions (13a,b,c) leads to the following variational problem without auxiliary conditions for Hamiltons operator H:

$$H \equiv \ell\ \tilde{H} = \ell\ (\ \tilde{C}_d + \lambda^{(1)}\tilde{C}_\ell + \lambda^{(2)}\tilde{C}_m + \sum_{t=1}^{N} \lambda_t \tilde{F}_t\ ) \tag{26}$$

In this formula $\lambda^{(1)}$, $\lambda^{(2)}$ and λ_t denote Lagrange's multipliers.

The extremum of H is obtained by vanishing its first variation ($\delta H = 0$). By cancellation of the coefficients of each independent variation $\delta\tilde{w}_{\theta\delta}$ the following equations are obtained

$$\sum_{n=1}^{N}\sum_{j=0}^{n-1}\left[\tilde{\Omega}_{n,\theta+\sigma+1,\sigma,j} + \tilde{\Omega}_{\theta+\sigma+1,n,j,\sigma}\right]\tilde{w}_{n-j-1,j} +$$

$$\lambda^{(1)}\ \tilde{\Lambda}_{\theta+\sigma+1,\sigma} + \lambda^{(2)}\ \tilde{\Gamma}_{\theta+\sigma+1,\sigma} + \lambda_{\theta+\sigma+1}\ \tilde{\psi}_{\theta+\sigma+1,\sigma} = 0. \tag{27}$$

$(1 \leq \theta+\sigma+1 \leq N\ ,\ \theta = 0,1,\ldots, (N-1)\ )$

These equations together with the auxiliary conditions (22),(23) and (24) form a linear algebraic system of equations which determines uniquely the optimum values of the coefficients $\tilde{w}_{\theta\sigma}$ as well as the Lagrange's multipliers $\lambda^{(1)}$, $\lambda^{(2)}$ and λ_t.

The variational problem concerning the optimization of the thin integrated delta wing component, for a given value of the similarity parameter ν is solved.

VI. Determination of the Optimum Shape of the Thick-Symmetrical Integrated Delta Wing

The determination of the optimum shape of the thick-symmetrical integrated delta wing component leads to the determination of the values of the coefficients $\tilde{w}^*_{ij}$ and $\bar{w}^*_{ij}$ in such a manner that the drag coefficient C^*_d attains its minimum and the auxiliary conditions (14a,b),(15),(16a,b,c),(17a,b) are satisfied.

The equations of the surface $\tilde{Z}^*$ and $\bar{Z}^*$ of the thick-symmetrical transformed integrated delta wing are obtained from downwashes $\tilde{w}^*$ and $\bar{w}^*$ as follows

$$\tilde{Z}^* = \int \tilde{w}\ d\tilde{x}_1 + \tilde{f}(\tilde{x}_2)\quad ,\quad \bar{Z}^* = \int \bar{w}\ d\tilde{x}_1 + \bar{f}(\tilde{x}_2) \tag{28a,b}$$

The arbitrary functions $\tilde{f}(x_2)$ and $\bar{f}(x_2)$ are determined in such a manner that the auxiliary conditions (17a,b) are satisfied. The equations of the surfaces $\tilde{Z}^*$ and $\bar{Z}^*$ of the transformed, thick-symmetrical integrated delta wing take the following forms

$$\tilde{Z}^* = -\sum_{m=1}^{N}\sum_{k=0}^{m-1} \frac{\tilde{w}^*_{m-k-1,k}}{m-k}\ |\tilde{x}_2|^k\ (1-\tilde{x}_1^{m-k}) \tag{29}$$

$$\bar{Z}^* = -\sum_{m=1}^{N}\sum_{k=0}^{m-1} \frac{\bar{w}^*_{m-k-1,k}}{m-k}\ |\tilde{x}_2|^k\ (1-\tilde{x}_1^{m-k}) \tag{30}$$

The conditions (17a,b) are now fulfilled and must be eliminated from the auxiliary conditions of the variational problem of the thick-symmetrical integrated delta wing. According to (2),(3),(6),(7),(9) and (4b) the remaining auxiliary conditions (14)-(16) can be written for the transformed thick-symmetrical integrated delta wing component in the following form:

- the cancellation of the thickness of the wing along its leading edges is of the form

$$\tilde{E}_t \equiv \sum_{m=t+1}^{N}\sum_{k=0}^{m-1} \tilde{a}^{(t)}_{mk}\ \tilde{w}^*_{m-k-1,k} = 0 \tag{31}$$

$(t = 0,1,\ldots,(N-1)\ )$

and δ^j_i is Kroenecker's Symbol;

- the continuity of class C_1 of the surface along the junction line between the wing and the fuselage leads to the following relations

$$\tilde{E}_t \equiv \sum_{m=t+1}^{N}\sum_{k=0}^{m-1} \tilde{c}^{(t)}_{mk}\ (\tilde{w}^*_{m-k-1,k} - \bar{w}^*_{m-k-1,k}) = 0 \tag{32}$$

$(t = 0,1,\ldots, (N-1)\ )$

$$\tilde{G}_t \equiv \sum_{m=t+1}^{N}\sum_{k=0}^{m-1} \tilde{g}^{(t)}_{mk}\ (\tilde{w}^*_{m-k-1,k} - \bar{w}^*_{m-k-1,k}) = 0 \tag{33}$$

$(t = 0,1,\ldots, (N-1)\ )$

$$\tilde{L}_t \equiv \sum_{m=t+1}^{N}\sum_{k=0}^{m-1} \tilde{\ell}^{(t)}_{mk}\ (\tilde{w}^*_{m-k-1,k} - \bar{w}^*_{m-k-1,k}) = 0 \tag{34}$$

$(t = 0,1,\ldots, (N-1)\ )$

- the condition of given relative volume of the wing is of the form

$$\tilde{\tau} \equiv \sum_{m=1}^{N}\sum_{k=0}^{m-1} \tilde{\tau}_{mk}\ \tilde{w}^*_{m-k-1,k} = \tau_0\ \sqrt{\ell} \tag{35}$$

- the condition of given relative volume of the fuselage is of the form

$$\bar{\tau} \equiv \sum_{m=1}^{N}\sum_{k=0}^{m-1} \bar{\tau}_{mk}\ \bar{w}^*_{m-k-1,k} = \tau'_0\ \sqrt{\ell} \tag{36}$$

The drag coefficient $\tilde{C}^*_d$ of the thick-symmetrical integrated transformed delta wing is of the form:

$$\tilde{C}^*_d = \sum_{n=1}^{N}\sum_{m=1}^{N}\sum_{k=0}^{n-1}\sum_{j=0}^{n-1}\Big[(\tilde{\Omega}^*_{nmkj}\ \tilde{w}^*_{n-j-1,j} + \tilde{\Omega}'^*_{nmkj}\ \bar{w}^*_{n-j-1,j})\ \tilde{w}^*_{m-k-1,k} + (\bar{\Omega}^*_{nmkj}\ \bar{w}^*_{n-j-1,j} + \tilde{\Omega}'^*_{nmkj}\ \tilde{w}^*_{n-j-1,j})\ \bar{w}^*_{m-k-1,k}\Big] \tag{37}$$

The coefficients $\tilde{a}^{(t)}_{mk}$, $\tilde{c}^{(t)}_{mk}$, $\tilde{g}^{(t)}_{mk}$, $\tilde{\ell}^{(t)}_{mk}$, $\tilde{\tau}_{mk}$, $\bar{\tau}_{mk}$ and $\tilde{\Omega}^*_{nmkj}$, $\tilde{\Omega}'^*_{nmkj}$, $\bar{\Omega}^*_{nmkj}$ and $\bar{\Omega}'^*_{nmkj}$ depend only on the similarity parameter ν (because $\bar{k} = \bar{\nu}/\nu$ is considered here constant).

The variational problem concerning the determination of the minimum of the drag functional C^*_d with the auxiliary conditions (14)-(16) leads to the variational problem without auxiliary conditions for Hamilton's operator

$$H^* \equiv \ell\ \tilde{H}^* = \ell(C^*_d + \mu^{(1)}\tilde{\tau} + \mu^{(2)}\bar{\tau}\ +$$

$$+ \sum_{t=1}^{N} (\mu_t \tilde{E}_t + \bar{\mu}_t \bar{E}_t + \eta_t \tilde{G}_t + \bar{\eta}_t \tilde{L}_t)) \quad (38)$$

In this formula $\mu^{(1)}$, $\mu^{(2)}$, μ_t, $\bar{\mu}_t$, η_t, $\bar{\eta}_t$ are Lagrange's multipliers. If the first variation of H^* is cancelled, i.e. the coefficient of each independent variation $\delta\tilde{w}_{\theta\sigma}$ and $\delta\bar{w}^*_{\theta\sigma}$ are annulated, the following equations are obtained:

$$\sum_{n=1}^{N} \sum_{j=0}^{n-1} \left[(\tilde{\Omega}^*_{n,\theta+\sigma+1,\sigma,j} + \tilde{\Omega}^*_{\theta+\sigma+1,n,j,\sigma}) \tilde{w}^*_{n-j-1,j} + (\tilde{\Omega}'^*_{n,\theta+\sigma+1,\sigma,j} + \bar{\Omega}^*_{\theta+\sigma+1,n,j,\sigma}) \bar{w}^*_{n-j-1,j} \right] +$$

$$\mu^{(1)} \tilde{\tau}_{\theta+\sigma+1,\sigma} + \sum_{t=1}^{N} (\mu_t \tilde{a}^{(t)}_{\theta+\sigma+1,\sigma} + \bar{\mu}_t \tilde{c}^{(t)}_{\theta+\sigma+1,\sigma} +$$

$$\eta_t \tilde{g}^{(t)}_{\theta+\sigma+1,\sigma} + \eta_t \tilde{\ell}^{(t)}_{\theta+\sigma+1,\sigma}) = 0 \quad (39)$$

and

$$\sum_{n=1}^{N} \sum_{j=0}^{n-1} \left[(\bar{\Omega}^*_{n,\theta+\sigma+1,\sigma} + \tilde{\Omega}'^*_{\theta+\sigma+1,n,j,\sigma}) \tilde{w}^*_{n-j-1,j} + (\bar{\Omega}'^*_{n,\theta+\sigma+1,\sigma,j} + \bar{\Omega}'^*_{\theta+\sigma+1,n,j,\sigma}) \bar{w}^*_{n-j-1,j} \right] +$$

$$\mu^{(2)} \bar{\tau}_{\theta+\sigma+1,\sigma} - \sum_{t=1}^{N} (\bar{\mu}_t \tilde{c}^{(t)}_{\theta+\sigma+1,\sigma} + \eta_t \tilde{g}^{(t)}_{\theta+\sigma+1,\sigma} +$$

$$\bar{\eta}_t \tilde{\ell}^{(t)}_{\theta+\sigma+1,\sigma}) = 0 \quad (40)$$

$(\theta = 0,1,2,\ldots, (N-1))$, $(1 \leq \theta+\delta+1 \leq N)$

These equations together with the auxiliary conditions (14)-(16) form a linear algebraic system of equations which determines uniquely the optimum values of the coefficients $\tilde{w}^*_{\theta\sigma}$ and $\bar{w}^*_{\theta\sigma}$ as well as the values of Lagrange's multipliers $\mu^{(1)}$, $\mu^{(2)}$, μ_t, $\bar{\mu}_t$, η_t and $\bar{\eta}_t$. The variational problem concerning the optimization of the thick-symmetrical integrated delta wing component (for a given value of ν) is solved.

VII. Determination of the Optimum-Optimorum Shape of the Thick, Lifting Integrated Delta Wing

The determination of the optimum-optimorum shape of the thick, lifting integrated delta wing reduces to the extremization of the total Hamilton's operator $H^{(t)}$

$$H^{(t)} \equiv \ell \tilde{H}^{(t)} = \ell(\tilde{H} + \tilde{H}^*). \quad (41)$$

Here H and H* represent Hamilton's operators for the thin and thick-symmetrical wing components of the transformed thick, lifting integrated delta wing and are given in (26) and (38). The extremum of $H^{(t)}$ is obtained by the vanishing of its first variation,

$$\delta H^{(t)} \equiv (\tilde{H}^{(t)} + \nu \frac{\partial H^{(t)}}{\partial \nu}) \delta\ell + \ell \sum_{\sigma=0}^{N-1} \sum_{\theta=0}^{N-\sigma-1} (\frac{\partial \tilde{H}}{\partial \tilde{w}_{\theta\sigma}} \delta\tilde{w}_{\theta\sigma} + \frac{\partial \tilde{H}^*}{\partial \tilde{w}^*_{\theta\sigma}} \delta\tilde{w}_{\theta\sigma} + \frac{\partial \tilde{H}^*}{\partial \bar{w}^*_{\theta\sigma}} \delta\bar{w}^*_{\theta\sigma}) = 0 \quad (42)$$

$(\theta = 0,1,2,\ldots, (N-1))$, $(1 \leq \theta+\sigma+1 \leq N)$

Taking into account that the variations $\delta\tilde{w}_{\theta\sigma}$, $\delta\tilde{w}^*_{\theta\sigma}$, $\delta\bar{w}^*_{\theta\sigma}$ and $\delta\ell$ are independent, it results in the equations

$$\tilde{H}^{(t)} + \nu \frac{\partial \tilde{H}^{(t)}}{\partial \nu} = 0 \quad (43)$$

$$\frac{\partial \tilde{H}}{\partial \tilde{w}_{\theta\sigma}} = 0 \quad (44)$$

$$\frac{\partial \tilde{H}^*}{\partial \tilde{w}^*_{\theta\sigma}} = 0 \quad , \quad \frac{\partial \tilde{H}^*}{\partial \bar{w}^*_{\theta\sigma}} = 0 \quad (45a,b)$$

$(\theta = 0,1,2,\ldots, (N-1))$, $(1 \leq \theta+\sigma+1 \leq N)$

The equations (44) and (45a,b) lead to the equations (27) and (39),(40) and the equation (43) is a coupling equation between the variational problems of the wing components (taken separately). The equations (27),(39),(40) and (43) together with the auxiliary conditions (22),(23),(24) and (32),(33),(35) and (36) form a non-linear transcendental system of equations, which can be used for the fully-analytical determination of the coefficients $\tilde{w}_{\theta\sigma}$, $\tilde{w}_{\theta\sigma}$ and $\bar{w}^*_{\theta\sigma}$ of the downwashes $\tilde{w}$, $\tilde{w}^*$ and $\bar{w}^*$ and also of the similarity parameters $\lambda^{(1)}$, $\lambda^{(2)}$, $\mu^{(1)}$, $\mu^{(2)}$, μ_t, $\bar{\mu}_t$, η_t and $\bar{\eta}_t$. The solution of this transcendental, non-linear system is very difficult to be directly found.

That is the reason that, instead of this original fully-analytical method, the author proposes the hybrid, numerical-analytical method (called also previously graphic-analytical method) which is better suited for the calculation on digital computers. The author has firstly proposed it in (2),(4),(5), generally formulated it in (6) and applied it for the design of the optimum-optimorum shape of the delta wing alone as in (6),(7),(8),(3).

Starting from the remark that, for each given value of the similarity parameter ν, this non-linear, transcendental system reduces to a linear algebraic system and a point of the limit line one can be obtained in a classical way.

Through systematical variation of the similarity parameter ν the entire limit line can be found in discrete form. The position of the limit line, which is numerically determined, represents the optimal value of the similarity parameter ν ($\nu = \nu_{opt}$) and the optimal thick, lifting integrated delta wing, which corresponds to this value of ν, is at the same time the optimum-optimorum thick, lifting integrated delta wing. As in Fig.4 the limit line for the thick, lifting integrated delta wing can be obtained through the addition of the ordinates of the limit lines of the thin and thick-symmetrical integrated delta wing components (for each given value of the similarity parameter ν).

According to the graphic-analytical method the solution of the non-linear, transcendental system of equations for the determination of the optimum-optimorum shape of the integrated wing (i.e. wing-fuselage configuration) leads to the solving of a set of linear algebraic systems as presented above.

The parameters which determine the shape of the optimum-optimorum integrated wing are:

- the optimal values of the similarity parameters ν and $\bar{\nu}$ ($\bar{\nu} = \bar{k}\nu$);
- the optimum-optimorum values of the coefficients $\tilde{w}_{\theta\sigma}$, $\tilde{w}^*_{\theta\sigma}$ and $\bar{w}^*_{\theta\sigma}$ of the downwashes $\tilde{w}$, $\tilde{w}^*$ and $\bar{w}^*$.

If in the non-linear, transcendental system of equations for the determination of the optimum-optimorum shape of the integrated wing the coefficients $\bar{w}_{\theta\sigma}$ and $\bar{\nu}$ are cancelled and the equations (32),(33),(34) and (36) are neglected, the non-linear, transcendental system of equations for the determination of the optimum-optimorum shape of the wing alone, previously given in (3),(6),(7), are obtained.

The optimum-optimorum wing alone (for the crui-

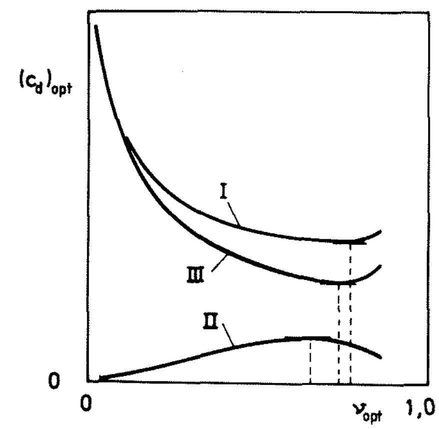

Fig.4 Limit Lines of Integrated Wing

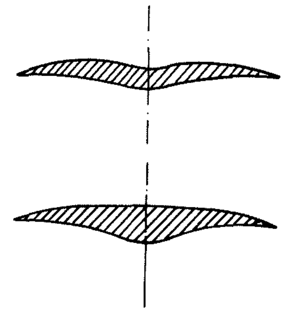

Fig.5 Transversal Sections of the Optimum-Optimorum Isolated and Integrated Wings

sing Mach number $M_\infty = 2$) has a convex shape in the vicinity of the apex and a wave form in the neighbourhood of the trailing edges. If the optimum-optimorum integrated delta wing is now taken into consideration the modification in the shape, due to the fuselage integration, is very important, as it can be observed in the Fig.5 for the transversal sections $x_1 = 0{,}6$ (at the same cruising Mach number $M_\infty = 2$).

VIII. Agreement with Experimental Results

In order to check the accuracy of this theory concerning the prediction of the aerodynamic characteristics, a wedged delta wing fitted with a conical fuselage, Fig.6, was tested in the frame work of a research contract*, by the author and collaborators**, in trisonic wind tunnel (section 60 x 60 cm^2) of the DFVLR-Köln***. The theoretically predicted values of the lift coefficient C_ℓ and pitching moment coefficient C_m according to the above theory are in very good agreement with the experimental results for the range of Mach numbers (M_∞ = 1,3 - 2,2) and angles of attack α ($|\alpha| < 20°$) taken here into consideration, as it is shown in Fig.(7a,b - 9a,b).

The dependences of lift- and pitching moment coefficients C_ℓ and C_m versus the angle of attack α are linear in supersonic flow also at higher angle of attack α as in Fig.7a,b and in [(23),(25)]. The variations of lift- and pitching moment coefficients C_ℓ and C_m with respect to the Mach number M_∞ are non-linear as it can be observed in Fig.(7a,b - 9a,b).

This agreement between theory and experiment is due to the accuracy of the solutions of the boundary value problems for the axial disturbance velocities $\tilde{u}$ and $\tilde{u}^*$ given in formulas (7) and (8).

These solutions for $\tilde{u}$ and $\tilde{u}^*$ present the following advantages in comparison with the ones obtained in the frame of slender body theory [(27),(28),(29),(30)]:

- they fulfil the full-linearised partial differential equation, which: is hyperbolic, includes the influence of Mach number M_∞ (in the similarity parameter ν) and does not need any restrictions concerning the magnitude of span;
- the boundary conditions along the characteristic surface, i.e., the Mach cone of the apex of the integrated wing, and at the infinity (forward) are satisfied;
- according to the hydrodynamic analogy of Carafoli [(12),(13)] the singularities in these solutions of u and u* are located only along the singular lines (i.e. along the leading edges of the wing, along the junction lines of the wing-fuselage configuration etc.) and therefore are easier to be applied as the solutions for axial disturbance velocities given in [(29),(30)], which are obtained by using singularities located on the whole wing surface;
- these singularities are chosen according to the principle of minimum singularities [(14),(15)] and therefore the potential solutions for u and u* given here are matched with a boundary layer solution (in the first approximation);
- the solutions (8) and (9) for u and u* can be also used for the calculation of pressure distribution and of aerodynamic characteristics of the wing-fuselage configurations given in discrete form. The surfaces of the wing and fuselage (i.e. $Z(x_1,x_2)$ and $\bar{Z}(x_1,x_2)$) can be piecewise approximated in form of polynomial expansions and the coefficients of downwashes w, w* and $\bar{w}^*$ are to be obtained by using the two-dimensional minimal quadratic error similar as in [(2),(33)];
- the time of calculation of the aerodynamic characteristics of the wing fitted with fuselage, by using

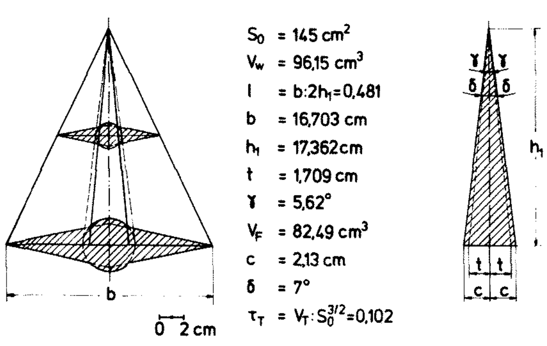

Fig.6 Delta Wing Fitted with Fuselage

*) supported by the Deutsche Forschungsgemeinschaft (DFG)

**) together with Dipl.-Ing. H. Esch, Dipl.-Ing. K. Feuerrohr (DFVLR), Ing. A. Scheich, Dipl.-Ing. D. Faliagas (Department of Aerodynamics of RWTH-Aachen)

***) Deutsche Forschungs- und Versuchsanstalt für Luft- und Raumfahrt (DFVLR)

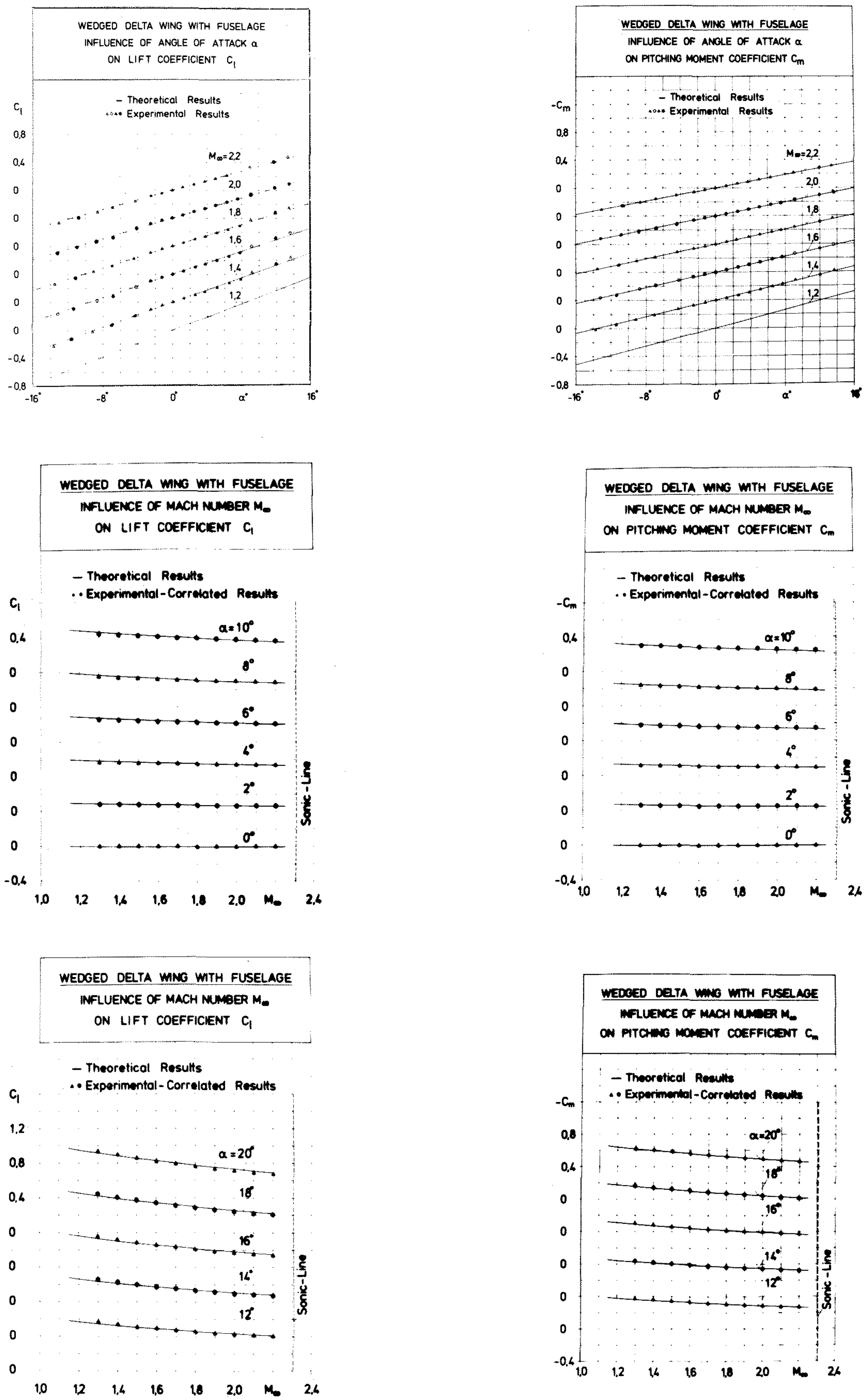

Fig. 7a,b - 9 a,b Agreement Between Theoretical and Experimental Determinated Aerodynamic Characteristics programmes according to this theory is less than 2 seconds on Cyber 175;

- the theoretical results concerning the determination of aerodynamic characteristics by using the formulas (8) and (9) for ũ and ũ* are in very good agreement with experimental results for a large range of supersonic Mach numbers and angles of attack because the supersonic flow remains attached to the wing and wing-fuselage configuration even at higher angle of attack α and at lower supersonic Mach number M_∞.

The theoretical predicted distribution of the pressure coefficient C_p according to this theory was also compared with experimental results for a large range of Mach numbers M_∞ and angles of attack α by the author and its collaborators as in (2),(9),(22),(24). The following results are obtained:

- at moderate angles of attack (cca. $|\alpha| < 10°$) and higher supersonic Mach numbers (cca. $M_\infty > 1,4$) the influence of leading edge vortices on pressure coefficient C_p can be neglected. This range of supersonic Mach numbers and angles of attack includes also the cruising flight for which the shape of supersonic transport aircraft is to be optimized. Therefore I have used the solutions (8) and (9) for ũ and ũ* as starting point for the fully-optimization of the shape of the surface of the integrated wing-fuselage configuration.
- At higher angles of attack ($10° < |\alpha| < 25°$) and lower supersonic Mach numbers ($1,25 < M_\infty < 1,4$) the influence of leading edge vortices on the pressure coefficient C_p occurs on the upper side of the wing in the region located in the vicinity of leading edges.

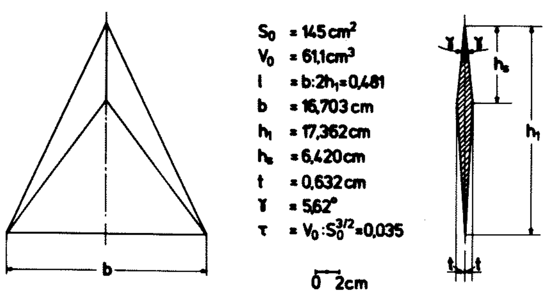

Fig.10 Double Wedged Delta Wing

In order to better predict the pressure coefficient C_p, including the effect of leading edge vortices, at lower supersonic Mach numbers and at higher angles of attack the author has recently obtained an approximated solution of Euler equations in spectral form by using the splitting technique and by including the solution for ũ and ũ* formerly given as modules in the expression of this generalised solution.

This generalised solution presents the advantages to be matched with the boundary layer solution and to converge to the linearised solutions (8) and (9) for ũ and ũ* for small perturbations (i.e. also at the infinity (forward)).

The comparison between the linearised and the generalised solutions can be used also for the determination of the intensity of leading edge vortices and for the estimation of the position of vortex core.

The optimum-optimorum integrated wing-fuselage configuration presents the following advantages:

- due to the optimization the drag is minimum (at cruising Mach number) and low for a large range of Mach numbers and angles of attack;
- due to the Kutta condition (13c) along its leading edges the induced drag disappears at cruising Mach number and is low for a large range of Mach numbers and angles of attack.

The leading edge vortices disappear (at cruising Mach number) and are of very small intensity for a large range of Mach numbers and angles of attack.

Another important consequence of the auxiliary condition (13c) is the gain in lift of the optimum-optimorum configurations presented here. In order to illustrate this property of the optimum-optimorum delta wing Adela, Fig.2, an äquivalent double wedged delta wing (i.e. a wing which has the same planpro-

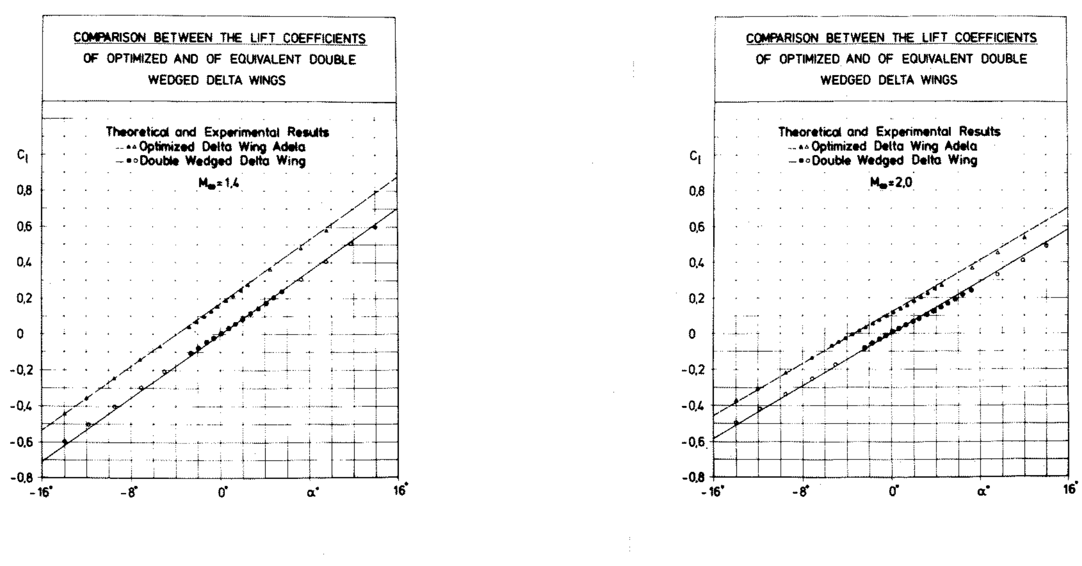

Fig. 11a,b Comparison between the Lift Coefficients of the Optimum-Optimorum Delta Wing Adela and of the Äquivalent Double Wedged Delta Wing jection and the same volume as the optimum-optimorum delta wing Adela) is also considered. (Fig.10)

The lift coefficients of these two wings are compared at the same conditions (i.e. at the same Mach numbers and angles of attack) the gain in lift of the optimum-optimorum delta wing Adela is very important as it can be seen in Fig.11a,b for the Mach numbers $M_\infty = 1{,}4$ and $M_\infty = 2{,}0$. The increasing in lift of the optimum-optimorum wings and wing-fuselage configurations due to the Kutta-condition on leading edges can be obtained only by a good suited coupling of each camber and twist of its skeleton surfaces as in (24).

- Due to the auxiliary conditions (32)-(34) the surface of the optimum-optimorum wing-fuselage configuration is integrated and looks like a wing alone. It allows also the partial or total integration of the engine nacelles inside the thickness of the integrated wing;
- last but not least, according to the optimum-optimorum theory of the author, all the geometrical characteristics (i.e. the distributions of cambers, twists, thicknesses and also the similarity parameters ν and $\bar{\nu}$ of the planprojections) of the optimum-optimorum integrated wing-fuselage configuration are simultaneously optimized. This simultaneity of optimization is very accurate. The succesive optimization of each single geometrical parameter of the configuration (by keeping the others constant) is inaccurate due to the interdependence of the geometrical parameters!

The optimum-optimorum theory is the single theory which allows the simultaneous optimization of all geometrical parameters of the surface and also of the planprojection of the wing-fuselage configuration. A good choice of the similarity parameters ν and $\bar{\nu}$ of the planprojections of the wing and of the fuselage plays an important role in the drag reduction as it can be observed in the Fig.4.

Conclusions

The hybrid analytical-numerical computational method for the determination of the optimum-optimorum shape of the integrated wing-fuselage configuration presents the following advantages:

- is accurate because it allows the simultaneous optimization of all the geometrical parameters of the wing-fuselage configuration;
- is the single method which give also the optimal geometrical parameters of the planprojection;
- is flexible, i.e. it allows, without difficulty, the addition or the suppression of some auxiliary conditions, the change of cruising Mach number (chosen for the optimization);
- is fast, the computation of the optimum-optimorum shape of the integrated wing-fuselage configuration needs 5 seconds computer time by Cyber 175.

The optimum-optimorum shape of the wing-fuselage configuration, proposed by the author, presents the following advantages:

- has reduced drag and high lift for a large range of Mach numbers and angles of attack;
- makes possible the total integration of aircraft configuration (the engine nacelles can be also easy integrated inside the thickness of the wing-fuselage configuration);

The very good and fast prediction of the aerodynamic characteristics of the optimized and non-optimized wing-fuselage configurations (also at higher angles of attack and lower supersonic Mach numbers) can be very useful for the calculation of the reentry of the space-shuttle in the earth atmosphere.

In conclusion, I propose the optimum-optimorum integrated wing-fuselage configuration for the design of future generation of integrated supersonic aircraft and space-shuttle.

References

1. NASTASE, A.: Forme Aerodinamice Optime prin Metoda Variationala (Optimum Aerodynamic Shape by Means of Variational Method). Ed. Acad. of Romania Bucharest, 1969, 240p., Chap. IV.
2. NASTASE, A.: Utilizarea Calculatorelor in Optimizarea Formelor Aerodinamice (Use of Computers in the Optimization of Aerodynamic Shapes). Ed. Acad. Romania Bucharest, 1973, 280p. Chap. I, III.
3. NASTASE, A.: Optimierte Tragflügelformen in Überschallströmungen. Braun Verlag Karlsruhe, 1986, 300p., Chap. III, IV.
4. NASTASE, A.: Eine graphisch-analytische Methode zur Bestimmung der Optimum-Optimorum Form dünner Deltaflügel in Überschallströmungen. RRST-MA* 1, 19, (1974).
5. NASTASE, A.: Eine graphisch-analytische Methode zur Bestimmung der Optimum-Optimorum Form symmetrisch-dicker Deltaflügel in Überschallströmungen. RRST-MA 19, (1974).
6. NASTASE, A.: Die Theorie des Optimum-Optimorum Tragflügels im Überschall. ZAMM 57 (1977).
7. NASTASE, A.: Modern Concepts for Design of Delta Wings for Supersonic Aircraft of Second Generation. ZAMM 59, (1979).
8. NASTASE, A.: New Concepts for Design of Fully-Optimized Configurations for Future Supersonic Aircraft. ICAS-Proceedings (1980), Munich.
9. NASTASE, A.: Validity of Solution of Three-Dimensional Linearised Boundary Value Problem for Axial Disturbance Velocity u, in Transonic - Supersonic Flow. ZAMM 65, (1985)
10. NASTASE, A.: Contribution à L'Etude des Formes Aerodynamiques Optimales. Faculté des Sciences de Paris en Sorbonne, 150p., 1970, Thèse.
11. GERMAIN, P.: La Théorie des Mouvements Homogènes et son Application au Calcul de Certaines Ailes Delta en Régime Supersonique. Rech. Aero., 7, 3-16, (1949).
12. CARAFOLI, E.: Asupra Caracterului Hidrodinamic al Solutiilor in Miscarile Conice Aplicate la Teoria Aripilor Poligonale. (About the Hydrodynamic Character of the Solutions of Conical Flow Used in the Theory of Polygonal Wings). Com. Acad. of Romania, Vol. II. (1952).
13. CARAFOLI, E., MATEESCU, D., NASTASE, A.: Wing Theory in Supersonic Flow. Pergamon Press, London, 1969, 590p., Chap. 4.
14. VAN DYKE, M.: Perturbation Methods in Fluid Mechanics. New York, Acad. Press, 1964.
15. NASTASE, A.: L'Etude du Comportement Asymptotique des Vitesses Axiales de Perturbation au Voisinage des Singularités. RRST-MA 4, 17, (1972).
16. NASTASE, A.: The Thin Delta Wing with Variable Geometry, Optimum for Two Supersonic Cruising Speeds. RRST-MA 3, 14, (1969).
17. NASTASE, A.: The Delta Wing of Symmetrical-Thickness with Variable Geometry, Optimum for Two Supersonic Cruising Speeds. RRST-MA 6, 15, (1970).
18. NASTASE, A.: Wing Optimization and Fuselage Integration for Future Generation of Supersonic Aircraft. Collection of Papers, 26th Israel Annual Conference on Aviation and Astronautics, (1984) and Israel Journal of Technology, Jerusalem (1985).
19. NASTASE, A.: Computation of Wing-Fuselage Configuration for Supersonic Aircraft. Preprints International Symposium on Computational Fluid Dynamics, Tokyo, 1985.

20. NASTASE, A.: Computation of Fully-Optimized Wing-Fuselage Configuration for Future Generation of Supersonic Aircraft. Integral Methods in Science and Engineering (Editors F. Payne, C. Corduneanu, A. Haji-Sheikh, T. Huang), Hemisphere Corporation, Washington D.C., 650p., 1986.
21. NASTASE, A.: Optimum-Optimorum Wing-Fuselage Integration in Transonic-Supersonic Flow. Proceedings of High Speed Aerodynamics, (Editor A. Nastase), 220p., Herchen Verlag Frankfurt, 1986.
22. NASTASE, A., BOZINIS, G., FALIAGAS, D.: Estimation of Position of Leading Edge Vortices on Wings at Higher Angle of Attack in Transonic-Supersonic Flow. Proceedings of High Speed Aerodynamics, (Editor A. Nastase), 220p., Herchen Verlag Frankfurt, 1986.
23. NASTASE, A., SCHEICH, A.: Theoretical Prediction of Aerodynamic Characteristics of Wings in Transonic-Supersonic Flow by Higher Angle of Attack and its Agreement with Experimental Results. GAMM 1986, Dortmund.
24. NASTASE, A., BOZINIS, G.: Experimental Determination of Position of Vortex Core at Higher Angle of Attack in Transonic-Supersonic Flow. GAMM 1986, Dortmund.
25. STOLLINGS, R.L., LAMB, M.: Wing Alone Aerodynamic Characteristics for High Angles of Attack at Supersonic Speeds. NASA Technical Paper 1889, (1981).
26. GRÖBNER, W., HOFREITER, N.: Integraltafel Springer-Verlag, 1975, 12-17p.
27. KÜCHEMANN, D.: The Aerodynamic Design of Aircraft. Pergamon Press, 1978, Chap. 5.
28. KEUNE, F., BURG, K.: Singularitätenverfahren der Strömungslehre. Braun Verlag Karlsruhe, 1975.
29. JONES, R., COHEN, D.: Aerodynamics of Wings at High Speeds. Princeton New Jersey, 1957, (Editors Donovan, A., and Lawrence, H.).
30. FERRARI, C.: Interaction Problems. Princeton New Jersey, 1957, (Editors Donovan, A., and Lawrence, H.).
31. SZEMA, K.Y., SHANKAR, V., RIBA, W.L., GORSKI, J.: Full Potential Treatment of Flows over 3-D Geometries Including Multibody Configurations. Preprints International Symposium on Computational Fluid Dynamics, Tokyo, 1985.
32. HOLST, T.L., THOMAS, S.D., KAYNAK, U., GUNDY, K.L., FLORES, J., CHADERJIAN, N.: Computational Aspects of Zonal Algorithms for Solving the Compressible Navier-Stokes Equations in Three Dimensions. Preprints International Symposium on Computational Fluid Dynamics, Tokyo, 1985.
33. NASTASE, A., STAHL, H.: Use of High Conical Flow Theory for the Determination of the Pressure Distribution on the Wave Rider and its Agreement with Experimental Results, for Supersonic Flow. ZAMM 61, (1981).
34. NASTASE, A., BOZINIS, G., BERTING, R.: Theoretical Determination of Pressure Coefficient C_p on Double Wedged Delta Wing and its Agreement with Experimental Results. ZAMM 65, (1985).

*) RRST-MA - Revue Roumaine des Sciences Techniques - Mécanique Applicée